

Supporting Information for:

Intelligent and Highly Sensitive Strain Sensor Based on Indium Tin Oxide Micromesh with High Crack Density

Yancong Qiao^{a*}, Hao Tang^a, Haidong Liu^a, Jinming Jian^b, Shourui Ji^b, Fei Han^c,
Zhiyuan Liu^c, Ying Liu^a, Yuanfang Li^a, Tianrui Cui^b, Jingxuan Cai^a, Guangyang Gou^b,
Bingpu Zhou^d, Yi Yang^b, Tian-Ling Ren^{b*}, and Jianhua Zhou^{a*}

^aSchool of Biomedical Engineering, Sun Yat-Sen University, Shenzhen, 518107, China.

^bSchool of Integrated Circuits (SIC) and Beijing National Research Center for Information Science and Technology (BNRist), Tsinghua University, Beijing, 100084, China.

^cCAS Key Laboratory of Human-Machine Intelligence-Synergy Systems, Shenzhen Institutes of Advanced Technology, Chinese Academy of Sciences (CAS), Shenzhen 518055, China

^dJoint Key Laboratory of the Ministry of Education, Institute of Applied Physics and Materials Engineering, University of Macau, Avenida da Universidade, Taipa, Macau 999078, China.

Email: zhoujh33@mail.sysu.edu.cn; rentl@tsinghua.edu.cn;
qiaoyc3@mail.sysu.edu.cn

Figure S1. The thickness of the ITO/PU micromesh measured by the profiler.

Figure S2. The transmittance at 4 points of ITO/PU micromesh during natural evaporation process.

Figure S3. The ITO/PU micromesh attached on the hand of tester for 10 h.

Figure S4. Relative resistance variation of IMSS after being wet.

Figure S5. The SEM of ITO/PU micromesh after the stress and recovering.

Figure S6. The SEM of ITO/PU micromesh after the bending and recovering.

Figure S7. Relative resistance variation of IMSS with the size of (12 mm*15 mm).

Figure S8. Relative resistance variation of IMSS with pre-stretching.

Figure S9. Relative resistance variation of IMSS packaged by the PU micromesh.

Figure S10. Relative resistance variation of IMSS packaged by the PU micromesh after attached on and peeled off from skin.

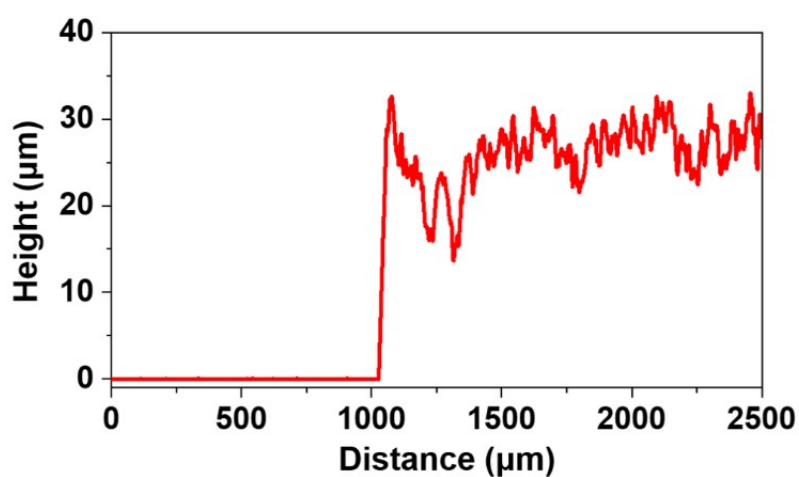


Figure S1. The thickness of the ITO/PU micromesh measured by the profiler.

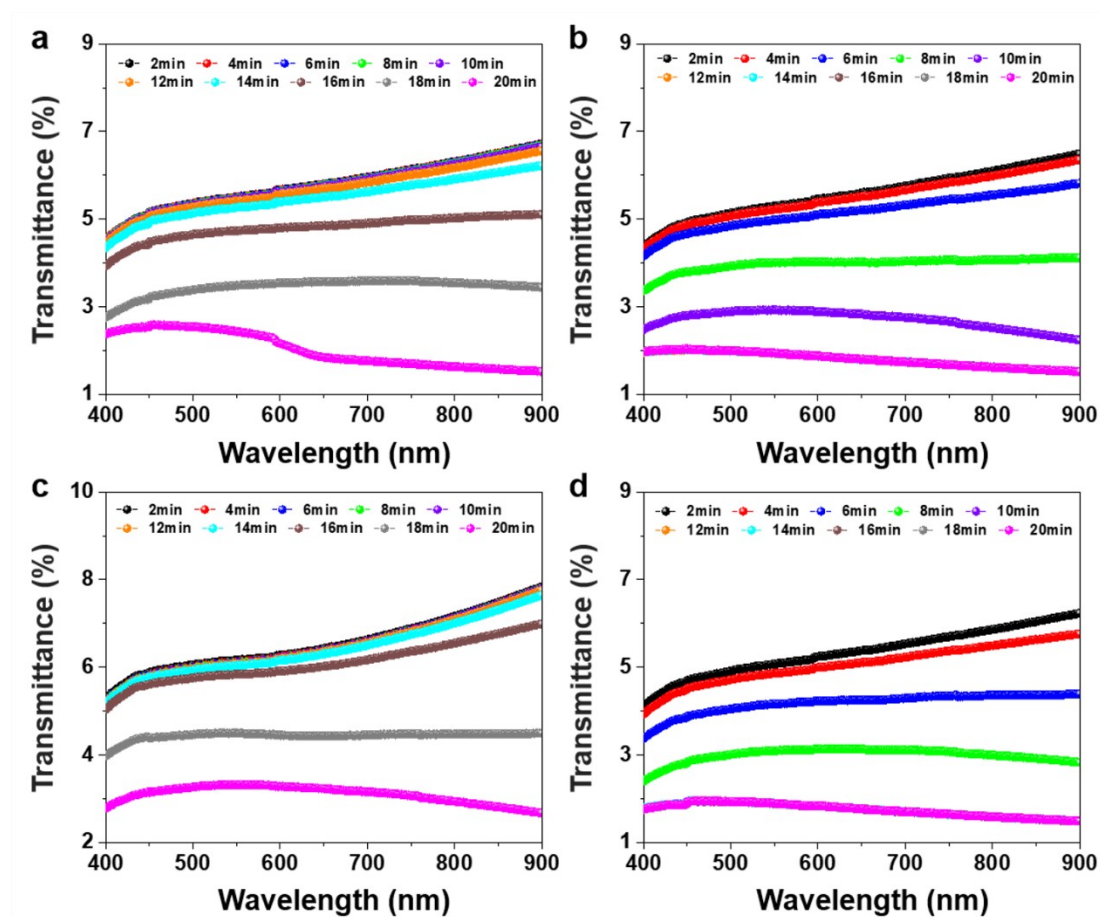


Figure S2. The transmittance at 4 points of ITO/PU micromesh during natural evaporation process.



Figure S3. The ITO/PU micromesh attached on the hand of tester for 10 h. After peeling off the micromesh, the skin has no adverse feeling.

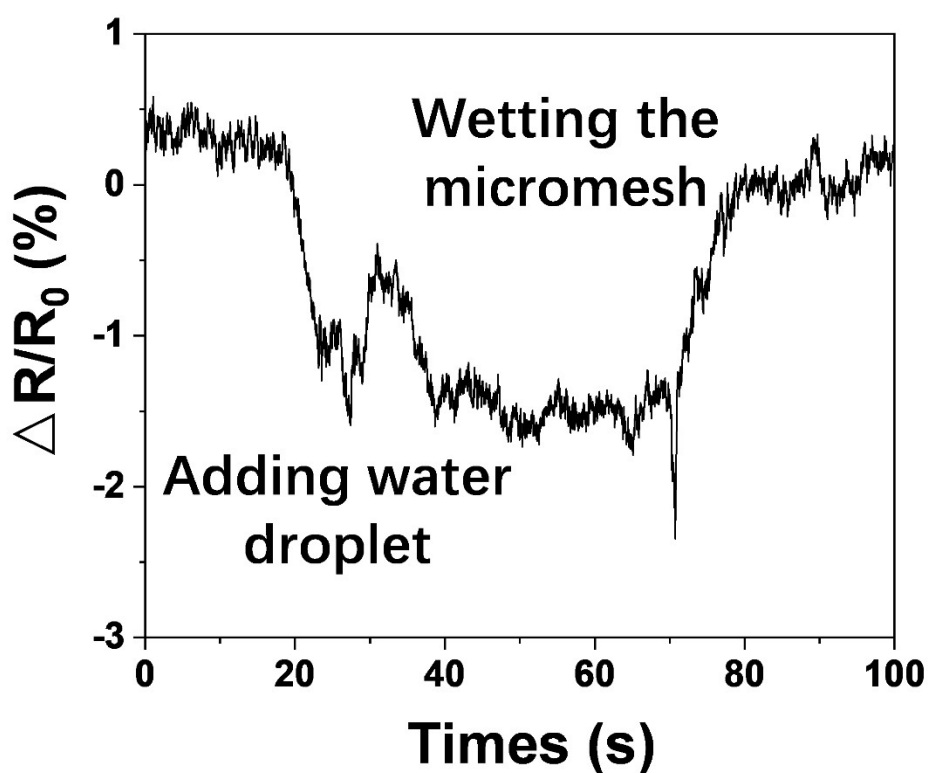


Figure S4. Relative resistance variation of IMSS after being wet. To eliminate the influence of stress. Another PU micromesh layer was used to package the IMSS. The water droplet was first dropped onto the packaged IMSS. Part of the droplet was absorbed leaving the other water wet the IMSS.

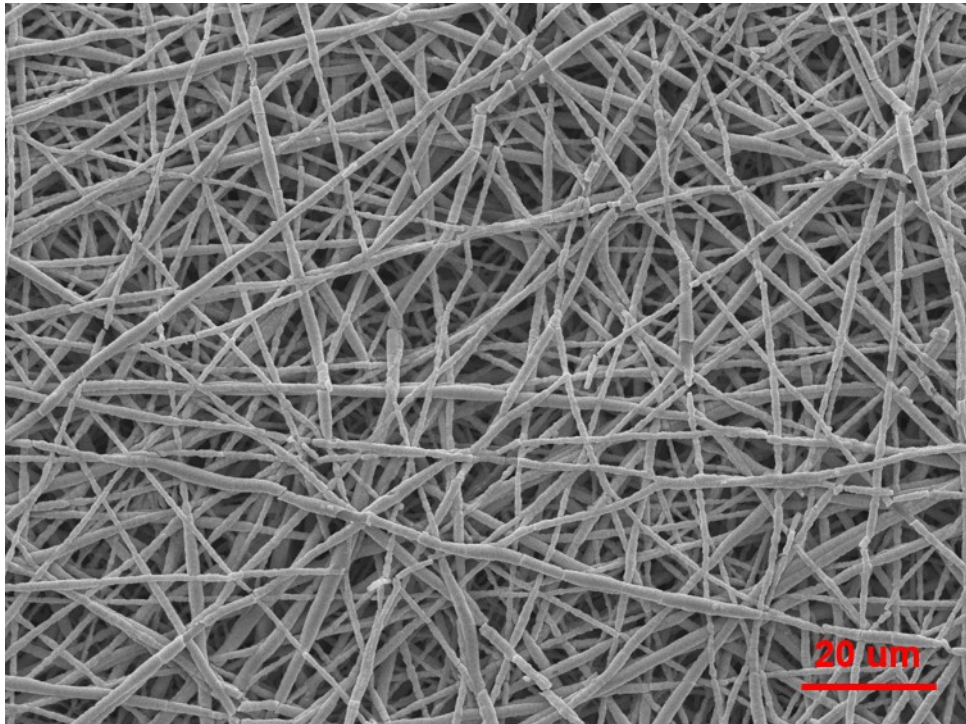


Figure S5. The SEM of ITO/PU micromesh after the stress and recovering.

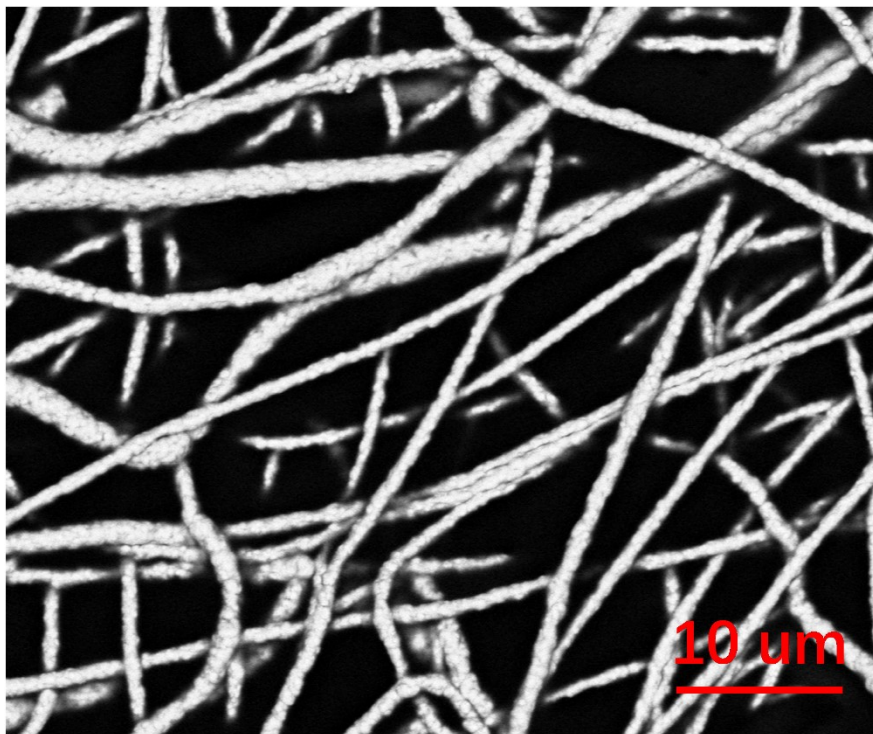


Figure S6. The SEM of ITO/PU micromesh after the bending and recovering.

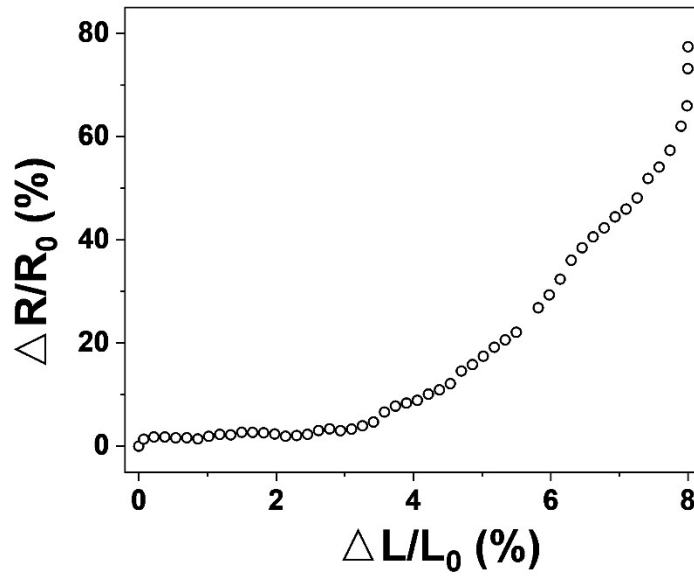


Figure S7. Relative resistance variation of IMSS with the size of (12 mm*15 mm) as a function of the tensile strain. The IMSS was stretched along longer side (15 mm).

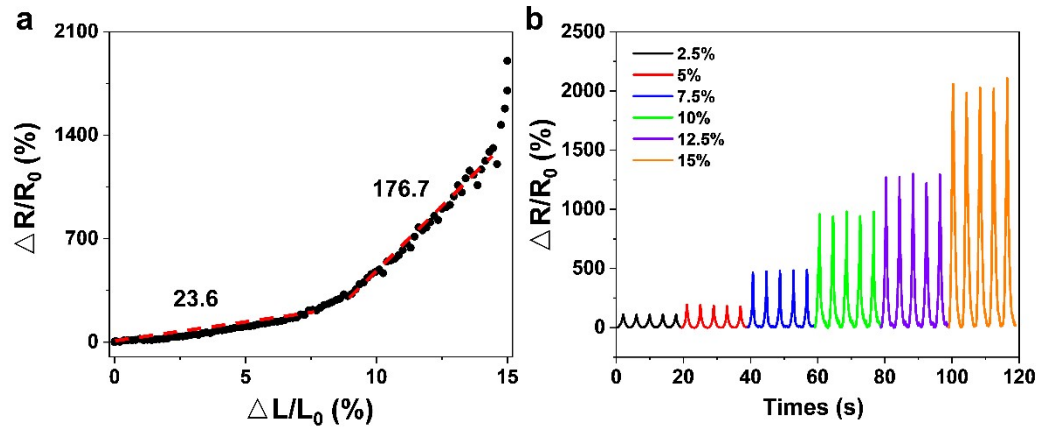


Figure S8. Relative resistance variation of IMSS with the size of (5 mm*16 mm) as a function of the tensile strain. The PU micromesh was stretched by 15% and sputtered. After the sputtering, the stress was released. The IMSS was stretched along longer side (16 mm). (b) Relative resistance variation of IMSS under tensile strains from 2.5% to 15%.

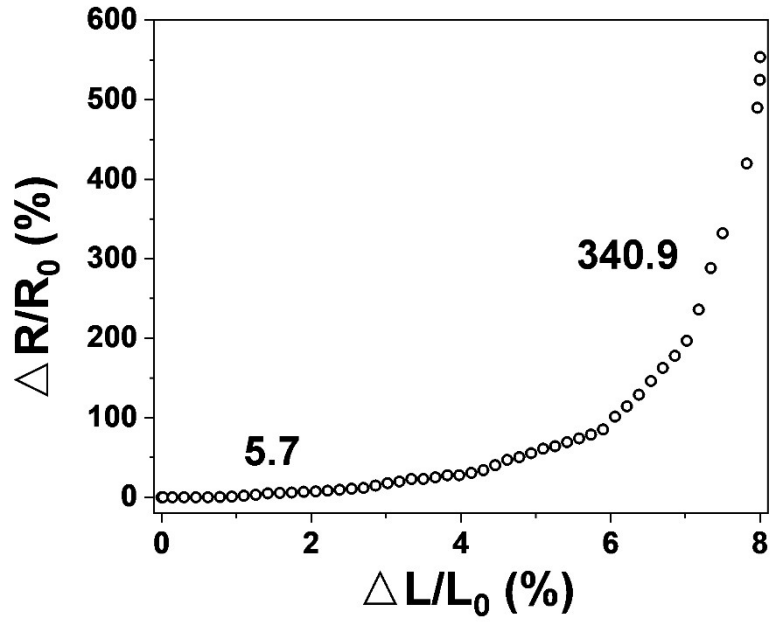


Figure S9. Relative resistance variation of IMSS packaged by the PU micromesh with the size of (12 mm*12 mm).

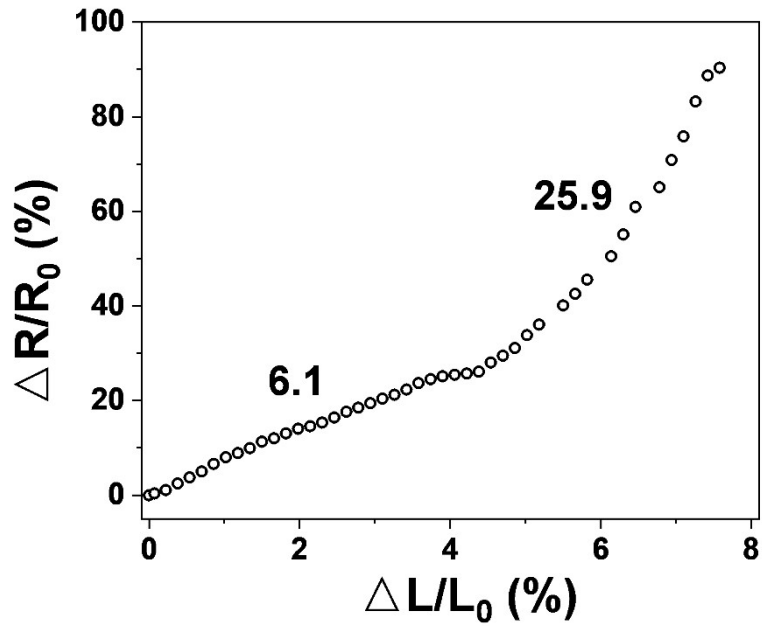


Figure S10. Relative resistance variation of IMSS packaged by the PU micromesh with the size of (12 mm*12 mm). After attached on the skin for 2 hours, the IMSS was peeled off and measured. During the attachment, the contour profile of IMSS is similar to the skin wrinkle. During the stress process, the wrinkle was first flattened which makes the IMSS has the lower GF.